

# Homogeneous Single-Component Betaine Ziegler–Natta Catalysts Derived from (Butadiene)zirconocene Precursors

GERHARD ERKER\*

Organisch-Chemisches Institut der Universität Münster,  
Corrensstrasse 40, D-48149 Münster, Germany

Received June 30, 2000

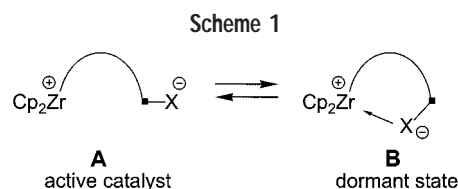
## ABSTRACT

(Butadiene)zirconocene adds  $B(C_6F_5)_3$  at a terminal diene carbon atom to yield the zirconocene-( $\mu$ -hydrocarbyl)-borate betaine  $Cp_2Zr[C_4H_6-B(C_6F_5)_3]$  (**4**). The dipolar complex **4** contains a distorted  $\pi$ -allyl moiety and features an additional stabilizing Zr–F–C(arene) coordination. Under kinetic control, an isomeric betaine system is formed, characterized by an internal  $Zr^+ \cdots CH_2[B]^-$  ion-pair interaction, that rearranges to **4** upon heating. A great variety of ansa-metallocene(butadiene) complexes and related systems cleanly form analogous metallocene-( $\mu$ -conjugated diene)-borate betaines upon treatment with  $B(C_6F_5)_3$  and related Lewis acids. Most of these systems represent very active homogeneous single-component Ziegler–Natta catalysts for  $\alpha$ -olefin polymerization and copolymerization. In addition, these betaine catalysts are ideally suited for carrying out mechanistic studies in active Ziegler–Natta catalyst systems. They allow for an experimental observation of the first alkene insertion step at the active single-component catalyst. This feature has been used for studying the mechanism of transfer of the stereochemical information from the bent metallocene backbone and for an experimental characterization of the energy profile of the alkene addition/alkene insertion reaction sequence in active homogeneous Ziegler–Natta systems. The neutral dipolar single-component catalysts (e.g., **4**) produce a polyolefin-modified  $R^-(CHR-CH_2)-C_4H_6-B(C_6F_5)_3^-$  counterion at the end of the initiation period upon entering into the repetitive active catalytic cycle.

## Introduction

Homogeneous metallocene Ziegler–Natta catalysts and related systems suited for  $\alpha$ -olefin polymerization and copolymerization have found much academic interest and have become of great practical importance in recent years.<sup>1</sup> The active chain propagating species of these catalysts are mostly group 4 metal alkyl cations (e.g.,  $^R Cp_2Zr-R^+$ )<sup>2</sup> that are formed by alkene insertion into initially generated active catalyst precursors. In group 4 metallocene cation chemistry, these are usually generated by treatment of a suitable precursor (e.g.,  $^R Cp_2Zr(CH_3)_2$ ) with a Brønsted acid (e.g.,  $R_3NH^+BAR_4^-$ ),<sup>3</sup> a Lewis acid (e.g.,  $B(C_6F_5)_3$ )<sup>4,5</sup> or another suitable alkyl anion abstractor (e.g.,

Gerhard Erker studied chemistry at the Universität Köln. He received his doctoral degree in 1972 (with W. R. Roth at the Universität Bochum). After doing postdoctoral research at Princeton University and the habilitation at the Universität Bochum, he was a Heisenberg fellow at the Max-Planck-Institut für Kohlenforschung in Mülheim. In 1985, he was appointed as a C3 professor of organic chemistry at the Universität Würzburg, and since 1990 he has been a C4 professor at the Universität Münster. His major current research interests are in the fields of organometallic chemistry and catalysis.



$[Ph_3C^+BAR_4^-]$ ,<sup>6</sup> or methylalumoxane  $[(MeAlO)_n]^-$ ,<sup>7</sup> that contain or generate low-nucleophilicity anions. Ion-pairs are probably formed (e.g.,  $[Cp_2ZrCH_3^+/CH_3B(C_6F_5)_3^-]$ )<sup>5</sup> in all these cases whose specific properties and catalytic features strongly depend on the specific conditions chosen for their generation. This situation complicates experimental studies in such systems to a great extent.

A less complicated situation can be envisioned where the active metallocene cation moiety and its supporting counteranion are combined in a single, then overall neutral molecule. In its open form (A) such a metallocene–hydrocarbyl–betaine system (see Scheme 1) represents an active metallocene Ziegler–Natta catalyst that will readily insert reactive 1-alkenes repeatedly, leading to an increasing separation of its cation and anion moieties until the system enters into the usual homogeneous Ziegler–Natta cycle by chain transfer. In the absence of an alkene, however, a stable dormant state (B) of the catalyst can be attained by internal ion-pairing. We have recently shown that systems of this general type are easily prepared<sup>8</sup> starting from readily available (butadiene)group 4 metallocene complexes.<sup>9</sup> The resulting betaines are very active single-component Ziegler–Natta catalyst systems for  $\alpha$ -olefin polymerization, which, in addition, are very well suited for carrying out mechanistic investigations. Some typical examples will be reviewed in this Account.<sup>10</sup>

## Synthesis and Structural Characterization of Zirconocene( $\mu$ -butadiene) $B(C_6F_5)_3$ Betaine Systems

A mixture of the (*s-cis*-) and (*s-trans*- $\eta^4$ -butadiene)ZrCp<sub>2</sub> isomers (**1**)<sup>9,11</sup> rapidly reacts with the organometallic Lewis acid  $B(C_6F_5)_3$ <sup>4</sup> in a 1:1 ratio to give a high yield of the metallocene( $\mu$ -butadiene) $B(C_6F_5)_3$  betaine complex **4**.<sup>8</sup> The X-ray crystal structure analysis (see Figure 1) shows the presence of a distorted monosubstituted  $\pi$ -allyl moiety at zirconium of (*E*)-configuration. The bulky  $B(C_6F_5)_3$  unit exhibits a chiral conformation that brings one of the ortho fluorine substituents close to the electrophilic zirconium center. The resulting Zr–F–C interaction ( $d$  Zr–F42 = 2.423(3) Å, angle Zr–F–C = 140.0(3)°) completes the coordination sphere of the bent metallocene in its major  $\sigma$ -coordination plane.<sup>12</sup>

The protective Zr–F–C interaction in the betaine complex **4** persists in solution although the system is highly dynamic. It undergoes a rapid  $\pi \rightleftharpoons \sigma \rightleftharpoons \pi$ -allyl interconversion<sup>13</sup> on the NMR time scale [ $\Delta G^\ddagger(313\text{ K}) = 19.8 \pm 0.4$  kcal/mol in toluene-*d*<sub>6</sub>] and exhibits dynamic

\* Fax: +49 251 8336503. E-mail: erker@uni-muenster.de.

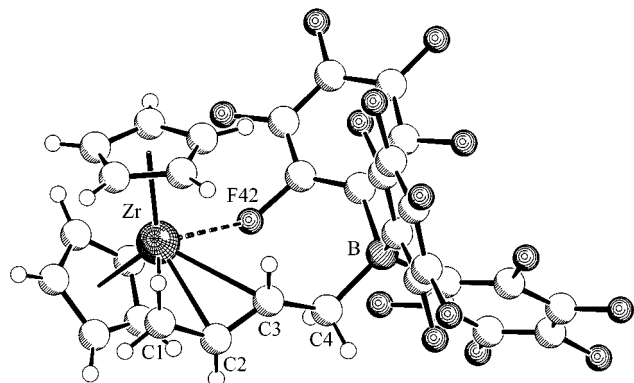


FIGURE 1. View of the molecular structure of the zirconocene( $\mu$ -butadiene) $B(C_6F_5)_3$  betaine complex **4**.

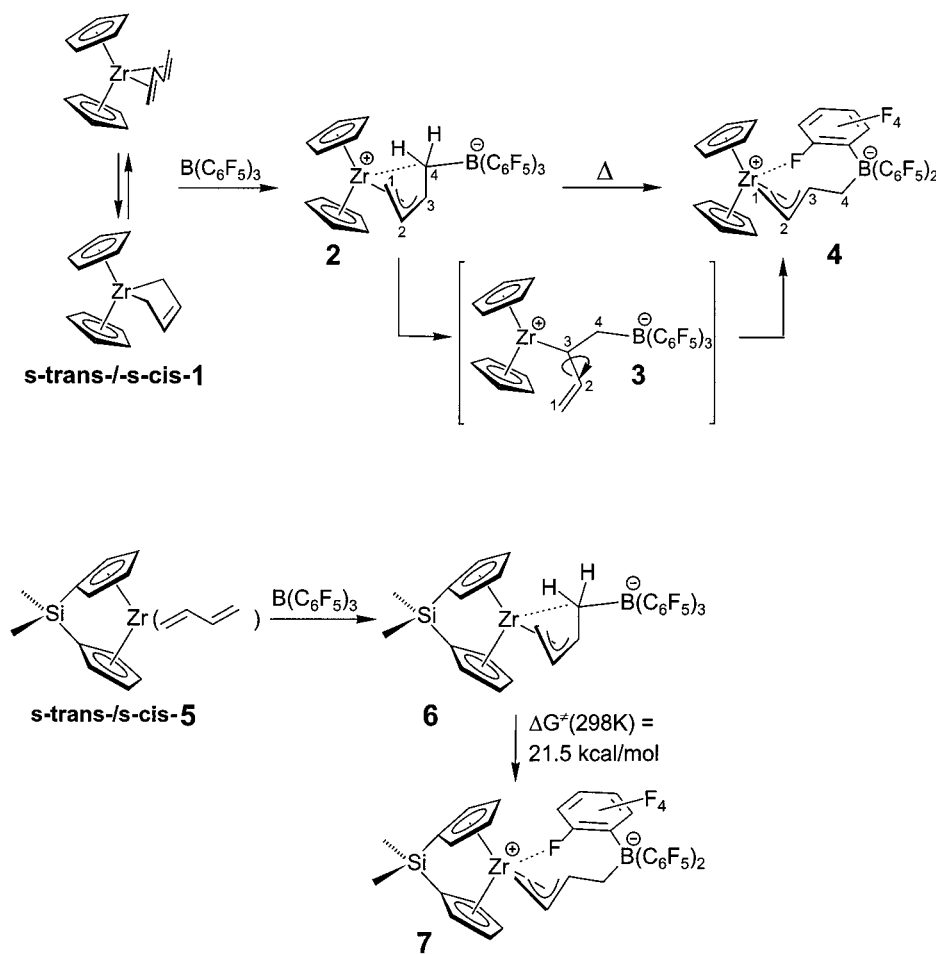
$^{19}F$  NMR spectra. At 213 K, the corresponding equilibration processes are frozen on the  $^{19}F$  NMR time scale (at 564 MHz), and complex **4** exhibits all its 15  $^{19}F$  NMR resonances separated. While the three *p*-F, the six *m*-F, and five of the *o*-F resonances appear in their typical range between  $\delta$   $-126.4$  and  $-137.5$ , the sixth ortho fluorine  $^{19}F$  NMR resonance is found shifted to an extremely negative  $\delta$  value of  $-213$ , indicating the occurrence of a divalent fluorine atom in **4**. Thus, the *o*-C–F–Zr interaction of the metallocene–betaine **4** is retained in solution. From the dynamic  $^{19}F$  NMR spectra, an activation energy of  $\Delta G^\ddagger$  (233 K) =  $8.1 \pm 0.4$  kcal mol $^{-1}$  was derived for the Zr–

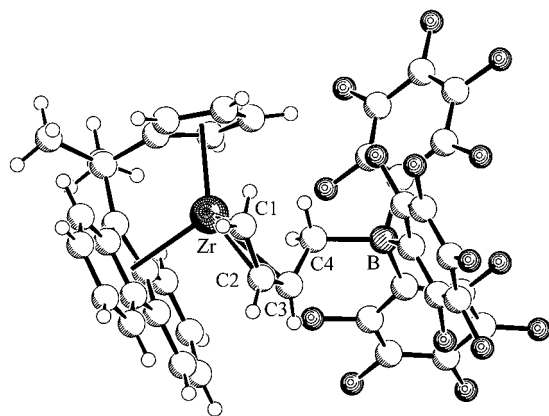
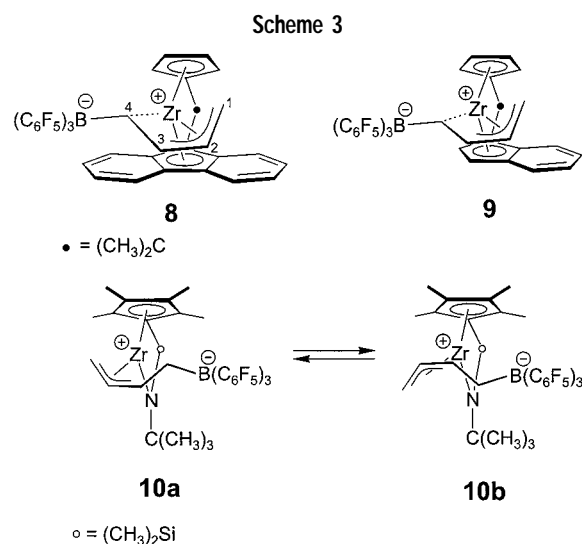
F(C) bond-breaking process, which is probably close to the Zr–F(C) bond dissociation energy in complex **4**.<sup>14</sup>

The  $\mu$ -F-bridged betaine complex **4** is the product of  $B(C_6F_5)_3$  addition to (butadiene)zirconocene under thermodynamic control. A structurally different betaine (**2**) is observed when the addition reaction is carried out under kinetic control at 213 K. Detailed NMR analysis and a comparison with analogous complexes that were characterized by X-ray diffraction (see below) have shown that the metallocene( $\mu$ -butadiene) $B(C_6F_5)_3$  isomer **2**, which exhibits a (*Z*)- $\eta^3$ -allyl unit, was formed initially, and may rearrange to the  $\mu$ -F-bridged (*E*)-allyl isomer (**4**) under conditions of thermodynamic control. This behavior was observed in a number of cases. Thus, the ansa-metallocene(butadiene) complex  $[Me_2Si(C_5H_4)_2]Zr(C_4H_6)$  (**5**) reacts with  $B(C_6F_5)_3$  at 233 K to yield the (*Z*)-betaine complex isomer **6**. At 298 K, it rearranges to the thermodynamically favored  $\mu$ -F-bridged (*E*)-allyl betaine isomer **7** in a thermally induced first-order process with a Gibbs activation energy of  $\Delta G^\ddagger$ (298 K) =  $21.5 \pm 0.2$  kcal mol $^{-1}$  (see Scheme 2).<sup>15</sup>

In a few cases, the (*Z*)-betaines are resistant to isomerization. Stable examples of such metallocene( $\mu$ -butadiene) $B(C_6F_5)_3$  complexes with (*Z*)-allyl configuration were isolated and characterized spectroscopically and by X-ray diffraction.<sup>15</sup> The betaine system **8** derived from the ansa-metallocene complex (*s-cis*- $\eta^4$ -butadiene) $[Me_2C(Cp)-$

Scheme 2



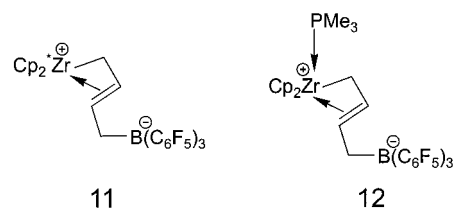
FIGURE 2. Molecular geometry of the betaine **8**.

(fluorenyl)Zr is a typical example. The X-ray crystal structure analysis of complex **8** (see Figure 2) shows a distorted (*Z*)- $\pi$ -allyl group [Zr–C1 2.322(2) Å, Zr–C2 2.506(3) Å, Zr–C3 2.545(3) Å] at zirconium. This ligand geometry brings carbon atom C4 of the hydrocarbyl chain into bonding contact with the metal atom [Zr–C4 2.542(3) Å] and leads to an orientation of the bulky  $\text{B}(\text{C}_6\text{F}_5)_3$  substituent away from the metallocene nucleus. The Zr–C(4)H<sub>2</sub>[B] contact probably must be regarded as an internal ion-pair interaction.

The related structure of the ansa-metallocene[ $\mu$ -C<sub>4</sub>H<sub>6</sub>-B(C<sub>6</sub>F<sub>5</sub>)<sub>3</sub>] betaine **9** was also established by X-ray diffraction. In this case it is remarkable that this singular stereoisomer was selectively formed out of the manifold of eight possible (*Z*)- and (*E*)-isomers under the applied reaction conditions. Butadiene complexes from the Me<sub>2</sub>-Si-linked-Cp\*/amido zirconium (“constrained geometry”) systems<sup>16,17</sup> also add B(C<sub>6</sub>F<sub>5</sub>)<sub>3</sub> to cleanly yield the respective (*Z*)-allyl betaines. In solution a 60:40 equilibrium mixture of the “prone” and “supine” isomers,<sup>18</sup> **10a** and **10b**, is obtained (see Scheme 3). Both show the *cis* <sup>3</sup>*J*(2-H, 3-H) coupling constants (**10a**, 9.3 Hz; **10b**, 9.8 Hz) typical of the [M]((*Z*)- $\mu$ -C<sub>4</sub>H<sub>6</sub>[B]) betaine isomers.

A third metallocene( $\mu$ -butadiene)B(C<sub>6</sub>F<sub>5</sub>)<sub>3</sub> betaine structural type is observed in cases where the metallocene is so bulky that the  $\text{—CH}_2\text{—B}(\text{C}_6\text{F}_5)_3$  terminus becomes con-

Scheme 4



formationally arranged away from the group 4 metal. Cp\*<sub>2</sub>-Zr[ $\eta^3$ -C<sub>3</sub>H<sub>4</sub>-CH<sub>2</sub>-B(C<sub>6</sub>F<sub>5</sub>)<sub>3</sub>] **11** is a typical example of such an open betaine system that exhibits a distorted  $\pi$ -allyl coordination (bond lengths Zr–C1 2.337 Å, Zr–C2 2.487 Å, Zr–C3 2.722 Å) (see Scheme 4).<sup>19</sup> The PMe<sub>3</sub> adduct (**12**) derived from the parent Cp<sub>2</sub>Zr( $\mu$ -C<sub>4</sub>H<sub>6</sub>)B(C<sub>6</sub>F<sub>5</sub>)<sub>3</sub> betaine (**4**) exhibits similar structural features.<sup>20</sup>

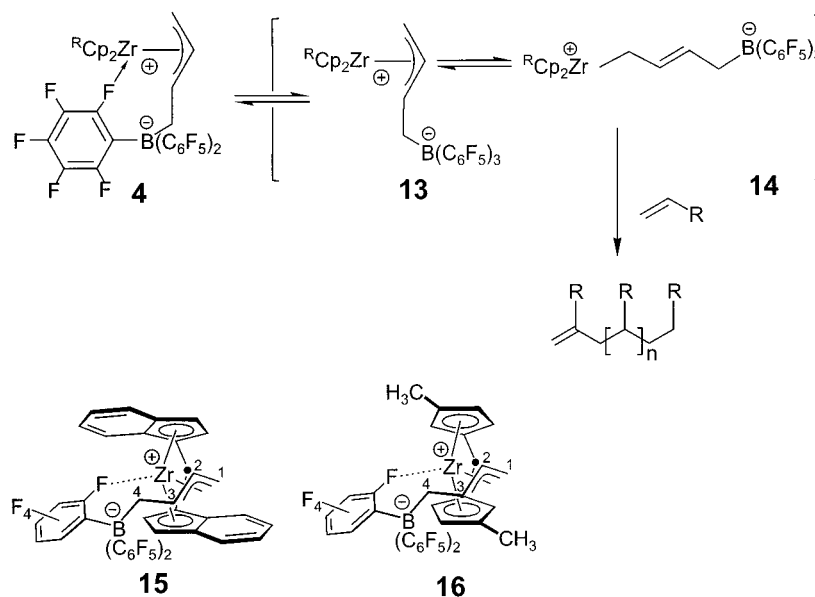
## Behavior in Catalytic Alkene Polymerization

The Cp<sub>2</sub>Zr( $\mu$ -C<sub>4</sub>H<sub>6</sub>)B(C<sub>6</sub>F<sub>5</sub>)<sub>3</sub> betaine system **4** behaves dynamically in solution (see above), which indicates a rapid equilibration, inter alia, with its open, non-fluorine-stabilized  $\sigma$ -allylmetallocene betaine isomer **14**. The latter is to be regarded as a neutral analogue of a ( $\sigma$ -allyl)ZrCp<sub>2</sub><sup>+</sup> cation and, consequently, should serve as an active metallocene betaine catalyst for  $\alpha$ -olefin polymerization as proposed and depicted in Scheme 1 (form A, see above). This is, indeed, the case: both ethene or propene are rapidly polymerized upon exposure to the Cp<sub>2</sub>Zr( $\mu$ -C<sub>4</sub>H<sub>6</sub>)B(C<sub>6</sub>F<sub>5</sub>)<sub>3</sub> betaine **4**.<sup>8</sup> More importantly, these alkenes are polymerized by a great variety of analogous metal-(butadiene)B(C<sub>6</sub>F<sub>5</sub>)<sub>3</sub> betaine systems, derived from the ansa-metallocene or “constrained geometry” frameworks that are typically used for the generation of very active and often selective homogeneous organometallic Ziegler–Natta catalysts. Typical examples include both the fluorine-bridged systems **7**, **15**, and **16** (see Schemes 2 and 5) and the carbon-coordinated betaines **8**–**10** (see Scheme 3). A comparison with conventionally generated catalysts (e.g., by treatment of the respective metallocene dichlorides with a large excess of methylalumoxane, see Table 1) has shown that the betaine catalyst systems are equally active and selective catalysts for the polymerization or copolymerization of  $\alpha$ -olefins.<sup>15</sup> Simple treatment of the (butadiene)metallocenes with B(C<sub>6</sub>F<sub>5</sub>)<sub>3</sub> thus leads to the formation of well-characterized single-component homogeneous Ziegler catalyst systems that can easily challenge the conventionally generated 1-alkene polymerization catalyst systems in their performance.

## Stoichiometric 1-Alkene Insertion

A variety of unsaturated reagents can be inserted in a 1:1 stoichiometry into the reactive zirconium–carbon bond of the <sup>R</sup>Cp<sub>2</sub>Zr( $\mu$ -C<sub>4</sub>H<sub>6</sub>)B(C<sub>6</sub>F<sub>5</sub>)<sub>3</sub> betaines. These reactions probably proceed via the  $\sigma$ -allyl betaine isomer **14** and thus mimic the first insertion step at an active metallocene Ziegler–Natta catalyst. A typical example is the reaction of **4** with ethene. At  $\text{—}35^\circ\text{C}$ , a selective monoinsertion is observed to generate complex **17a**,<sup>21</sup> which reacts further with ethene at higher temperatures to eventually produce

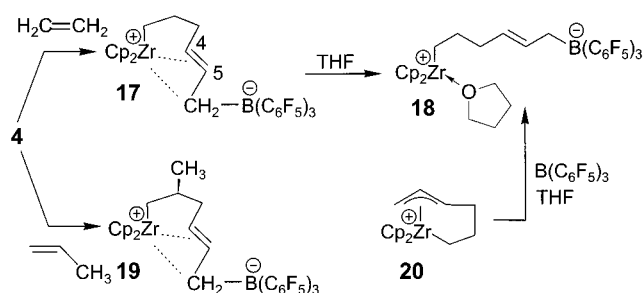
Scheme 5

**Table 1. Ethene and Propene Polymerization with Single-Component Betaine Ziegler–Natta Catalysts and Related Systems<sup>a</sup>**

metallocene/activator	catalyst	B/Zr (Al/Zr)	alkene <sup>b</sup>	activity <sup>c</sup>	% mmmm
[Me <sub>2</sub> Si(C <sub>5</sub> H <sub>4</sub> ) <sub>2</sub> ]Zr(C <sub>4</sub> H <sub>6</sub> )/B(C <sub>4</sub> F <sub>5</sub> ) <sub>3</sub>	<b>7</b>	1.05	E	1550	
[Me <sub>2</sub> Si(Ind) <sub>2</sub> ]Zr(C <sub>4</sub> H <sub>6</sub> )/B(C <sub>4</sub> F <sub>5</sub> ) <sub>3</sub>	<b>15</b>	1.24	E	2300	
		1.24	P	1220	78
[Me <sub>2</sub> Si(Ind) <sub>2</sub> ]ZrCl <sub>2</sub> /MAO		(1800)	P	6700	69
[Me <sub>2</sub> Si(3-MeC <sub>5</sub> H <sub>3</sub> ) <sub>2</sub> ]Zr(C <sub>4</sub> H <sub>6</sub> )/B(C <sub>4</sub> F <sub>5</sub> ) <sub>3</sub>	<b>16</b>	1.03	E	3370	
		1.03	P	240	85
[Me <sub>2</sub> Si(C <sub>5</sub> Me <sub>4</sub> )N <sup>t</sup> Bu]Ti(C <sub>4</sub> H <sub>6</sub> )/B(C <sub>4</sub> F <sub>5</sub> ) <sub>3</sub>	<b>10c</b>	1.03	E <sup>d</sup>	390	
[Me <sub>2</sub> C(C <sub>5</sub> H <sub>4</sub> )(Ind)]Zr(C <sub>4</sub> H <sub>6</sub> )/B(C <sub>6</sub> F <sub>5</sub> ) <sub>3</sub>	<b>9</b>	1.21	E	340	
[Me <sub>2</sub> C(C <sub>5</sub> H <sub>4</sub> )(Ind)]ZrCl <sub>2</sub> /MAO		(1065)	E	410	
[Me <sub>2</sub> C(C <sub>5</sub> H <sub>4</sub> )(Ind)]Zr(C <sub>4</sub> H <sub>6</sub> )/B(C <sub>6</sub> F <sub>5</sub> ) <sub>3</sub>	<b>9</b>	1.21	P	450	10
[Me <sub>2</sub> C(C <sub>5</sub> H <sub>4</sub> )(Ind)]ZrCl <sub>2</sub> /MAO		(1065)	P	220	10
[Me <sub>2</sub> C(C <sub>5</sub> H <sub>4</sub> )(Flu)]Zr(C <sub>4</sub> H <sub>6</sub> )/B(C <sub>6</sub> F <sub>5</sub> ) <sub>3</sub>	<b>8</b>	1.10	E	114	
[Me <sub>2</sub> C(C <sub>5</sub> H <sub>4</sub> )(Flu)]ZrCl <sub>2</sub> /MAO		(1117)	E	147	
[Me <sub>2</sub> C(C <sub>5</sub> H <sub>4</sub> )(Flu)]Zr(C <sub>4</sub> H <sub>6</sub> )/B(C <sub>6</sub> F <sub>5</sub> ) <sub>3</sub>	<b>8</b>	1.10	P	300	73 <sup>e</sup>
[Me <sub>2</sub> C(C <sub>5</sub> H <sub>4</sub> )(Flu)]ZrCl <sub>2</sub> /MAO		(1117)	P	240	82 <sup>e</sup>

<sup>a</sup> Reactions at 40 °C in toluene, unless indicated. <sup>b</sup> E = ethene, P = propene. <sup>c</sup> In grams of polymer per millimole of [Ti/Zr] per hour per bar. <sup>d</sup> Reaction at 90 °C. <sup>e</sup> Syndiotactic rrrr pentad.

Scheme 6

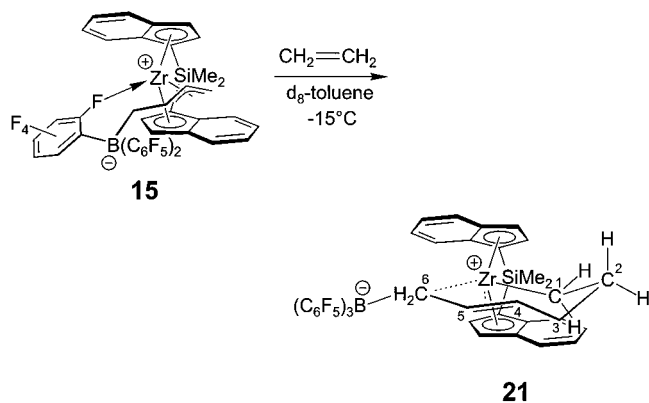


polyethylene (see Scheme 6). The ethene insertion reaction pauses at the stage of formation of the reactive monoinsertion product under suitable conditions<sup>22</sup> because it features a specific intramolecular stabilization of the reactive metallocene cation moiety by means of a weak internal coordination of the C(4)=C(5) carbon–carbon double bond *and* an internal zirconium/carbon ion-pair interaction with the adjacent –CH<sub>2</sub>–[B] unit. This combined weak interaction is sufficient to make the reactive

mono-ethene insertion product just observable by NMR spectroscopy under suitable conditions at low temperature. The internal ( $\pi$ -alkene)Zr coordination of **17** can readily be recognized from the resulting typical <sup>13</sup>C NMR features, taking the THF-opened derivative as a reference. The C4 <sup>13</sup>C NMR signal of **17** is shifted to a substantially larger  $\delta$  value of 146.4 (**18**:  $\delta$  127.9;  $\Delta\delta$  +21.5), whereas the C5 resonance shows the opposite behavior due to complexation (**17**:  $\delta$  123.6;  $\Delta\delta$  = –13.7). This typical behavior probably arises due to the polar structure of the ( $\pi$ -alkene)Zr<sup>+</sup> structural unit.<sup>23</sup>

A variety of 1-alkene homologues was also inserted.<sup>21</sup> Regioselective incorporation of these reagents was observed to generate the primary monoinsertion products (e.g., **19**) that exhibit alkyl substitution at carbon atom C2 of the resulting hydrocarbon chain. Thus, stoichiometric 1-alkene insertion at the metallocene betaines **4** mimics the favored regioselective [1,2]insertion behavior that is usually observed during  $\alpha$ -olefin polymerization in reactive metallocene Ziegler–Natta catalyst systems.<sup>1</sup>

Scheme 7



## Mechanistic Studies

**I. Monitoring the Stereochemistry of the First 1-Alkene Insertion Step on an Active Metallocene Catalyst.** 1-Alkene polymerization on chiral ansa-metallocene Ziegler–Natta catalysts can be very stereoselective. The  $M(\mu\text{-C}_4\text{H}_6)\text{B}(\text{C}_6\text{F}_5)_3$  single-component catalysts containing such chiral metallocene moieties should be suitable systems for direct experimental observation of the stereochemistry of 1-alkene insertion.

We have used the  $[\text{rac-Me}_2\text{Si}(\text{indenyl})_2]\text{Zr}(\mu\text{-C}_4\text{H}_6)\text{B}(\text{C}_6\text{F}_5)_3$  system **15** for this study.<sup>24</sup> Treatment of **15** with ethylene at  $-15^\circ\text{C}$  in toluene- $d_8$  led to the formation of a single monoinsertion product (**21**), which is again characterized by weak internal alkene coordination to zirconium ( $^1\text{H}$  NMR: 4-H, 5-H,  $\delta$  5.41 and 5.87,  $\text{trans } ^3J(4\text{-H}, 5\text{-H}) = 15.7$  Hz) and an internal ion-pair interaction between Zr and the terminal  $-\text{CH}_2\text{-[B]}$  moiety. The reaction of **15** with ethene can lead, in principle, to the formation of two diastereomers with relative configurations ( $M^*$ )(4,5,6- $pR^*$ ) or ( $M^*$ )(4,5,6- $pS^*$ ). Apparently, only one of these stereoisomers is selectively formed in the CC coupling reaction at the front side of the chiral bent metallocene (see Scheme 7).

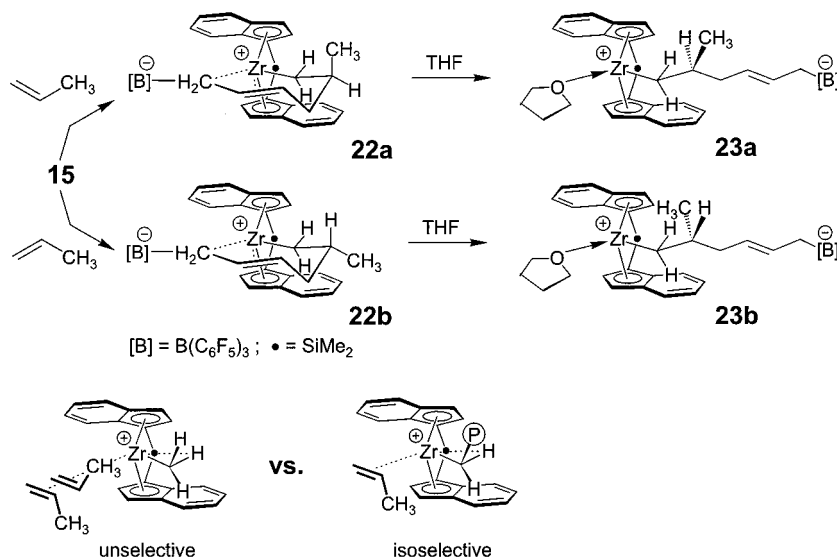
Treatment of **15** with propene at 253 K in toluene- $d_8$  resulted in the formation of a 60:40 mixture of the two

diastereoisomers **22a** and **22b**, which are distinguished by the relative configuration of the newly formed chiral carbon center C2. This was secured by treatment with the donor ligand THF- $d_8$ , leading to displacement of the coordinated alkene moiety ( $\text{C}_4=\text{C}_5$ ) from the metal center to yield a mixture of the products **23a** and **23b**, again in a 60:40 ratio. We have seen (see above) that highly isotactic polypropylene is formed at the chiral ansa-metallocene betaine catalyst **15** (>90% mmmm at 253 K). Thus, the stereochemistry of the chiral  $C_2$ -symmetric ansa-metallocene backbone of the catalyst **15** is very effectively transferred through each of the alkene inserting carbon–carbon coupling steps, *except* for the very first insertion leading to **22**. This behavior is similar to what was previously observed in classical heterogeneous Ziegler–Natta catalysis.<sup>25</sup> This observation indicates that the stereochemistry is not transferred directly from the bent metallocene backbone onto the incoming prochiral alkene, but that a stereochemical relay is involved to achieve an effective Re/Si discrimination. In view of our experiments and those done by others,<sup>26</sup> it is likely that an auxiliary chirality center generated by an  $\alpha$ -agostic metal–H–C interaction plays this role in the active isoselective metallocene  $\alpha$ -olefin polymerization catalysts (see Scheme 8).

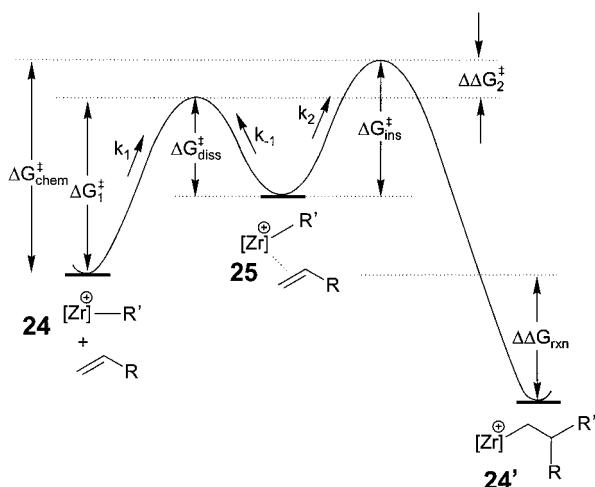
**II. Experimental Characterization of the Alkene Addition/Alkene Insertion Energy Profile in Single-Component Betaine Ziegler–Natta Catalyst Systems.** In essence, the alkene polymerization process on a homogeneous Ziegler–Natta catalyst contains a nearly continuous repetition of two consecutive steps, namely alkene coordination to the metal (rate constants  $k_1[\text{monomer}]$ ; reverse alkene dissociation,  $k_{-1}$ ) followed by alkene insertion (rate constant  $k_2$ ) (see Scheme 9). Which of the two transition states lies higher and, thus, which of the two parts of the overall reaction is rate and/or selectivity determining has not yet been resolved experimentally from a catalytic Ziegler–Natta polymerization cycle.<sup>27</sup>

The single alkene insertion of the metallocene betaine

Scheme 8



Scheme 9



system **4** to give **19** probably provides a very good image of the respective two-stage polymerization process that will allow for a quantitative evaluation of the typical reaction profile involved in such reactions. The ( $\pi$ -alkene)-( $\sigma$ -allyl)metallocene betaine complex **27** seems to be the essential reactive intermediate in the initiation phase on these single-component Ziegler–Natta catalysts. Complex **27** can undergo either of two competing processes which mimic the reaction steps that characterize the energy profile depicted in Scheme 9, namely alkene insertion ( $k_2$ ,  $\Delta G_{\text{ins}}^{\ddagger}$ ) to yield the experimentally observed product **19** or alkene dissociation ( $1/2 k_{-1}$ ,  $\Delta G_{\text{diss}}^{\ddagger}$ ). The latter reaction leads back to the starting betaine system **4** or to its enantiomer *ent*-**4** (see Scheme 10).<sup>28,29</sup>

In the absence of an olefin, the metallocene borate betaine complex **4** undergoes a thermally induced intramolecular enantiomerization reaction (**4**  $\rightleftharpoons$  *ent*-**4**) that probably involves the intermediate **26**. Its rate was determined by <sup>1</sup>H NMR magnetization transfer. In the presence of a 1-alkene, the observed rate of magnetic exchange

( $k_{\text{m(obs)}}$ ) is increased, probably because the  $\sigma$ -allylmetal-locene intermediate becomes stabilized by alkene coordination. A unique situation results, namely, that the ( $\pi$ -alkene)( $\sigma$ -allyl)metallocene intermediate **27**, which leads to enantiomerization, is at the same time the essential reactive intermediate of the (irreversible) alkene insertion reaction producing **19**. Thus, the rate of the observed magnetization transfer ( $k_{\text{m(obs)}}$ ) characterizing the reversible **4**  $\rightleftharpoons$  *ent*-**4** equilibration is dependent on the rate of the competing chemical reaction ( $k_{\text{chem}}$ , barrier  $\Delta G_{\text{chem}}^{\ddagger}$ ).<sup>28,29</sup> The analysis of this remarkable kinetic situation results in a simple pair of equations (eqs 1 and 2) that allows the determination of  $k_1$  and the  $k_2/k_{-1}$  ratio from the experimentally observed rate constants  $k_{\text{chem}}$  and  $k_{\text{m(obs)}}$ , which were both measured with a sufficient accuracy under suitable reaction conditions.<sup>29</sup>

$$(\Delta G_1^{\ddagger}): \quad k_1 = k_{\text{chem}} + 2k_{\text{m(obs)}} \quad (1)$$

$$(\Delta\Delta G_2^{\ddagger}): \quad \frac{k_2}{k_{-1}} = \frac{k_{\text{chem}}}{2k_{\text{m(obs)}}} \quad (2)$$

This allowed for a deconvolution of the observed overall activation barrier ( $\Delta G_{\text{chem}}^{\ddagger}$ ) of the two-step process. The activation barrier of the first step ( $\Delta G_1^{\ddagger}$ , i.e., the formation of the reactive intermediate **27**, could be separated from the transition-state energy of the actual alkene insertion step ( $\Delta\Delta G_2^{\ddagger}$ , see Scheme 8). The value of  $\Delta\Delta G_2^{\ddagger}$  obtained by this treatment can be positive or negative. If located not more than ca. 2 kcal/mol below the  $\Delta G_1^{\ddagger}$  value, a reasonably accurate determination appears feasible even in the latter case.

In a first experiment, (MeCp)<sub>2</sub>Zr(butadiene) (**1a**) was thus treated with B(C<sub>6</sub>F<sub>5</sub>)<sub>3</sub> to yield **4a**, and then propene was inserted to yield the product (MeCp)<sub>2</sub>ZrCH<sub>2</sub>CH(CH<sub>3</sub>)-C<sub>4</sub>H<sub>6</sub>B(C<sub>6</sub>F<sub>5</sub>)<sub>3</sub> (**19a**). The overall activation barrier amounts to  $\Delta G_{\text{chem}}^{\ddagger}(253 \text{ K}) = 17.1 \pm 0.1$  kcal/mol. The activation barrier of alkene addition ( $\Delta G_1^{\ddagger}(253 \text{ K}) = 16.5 \pm 0.5$  kcal/

Scheme 10

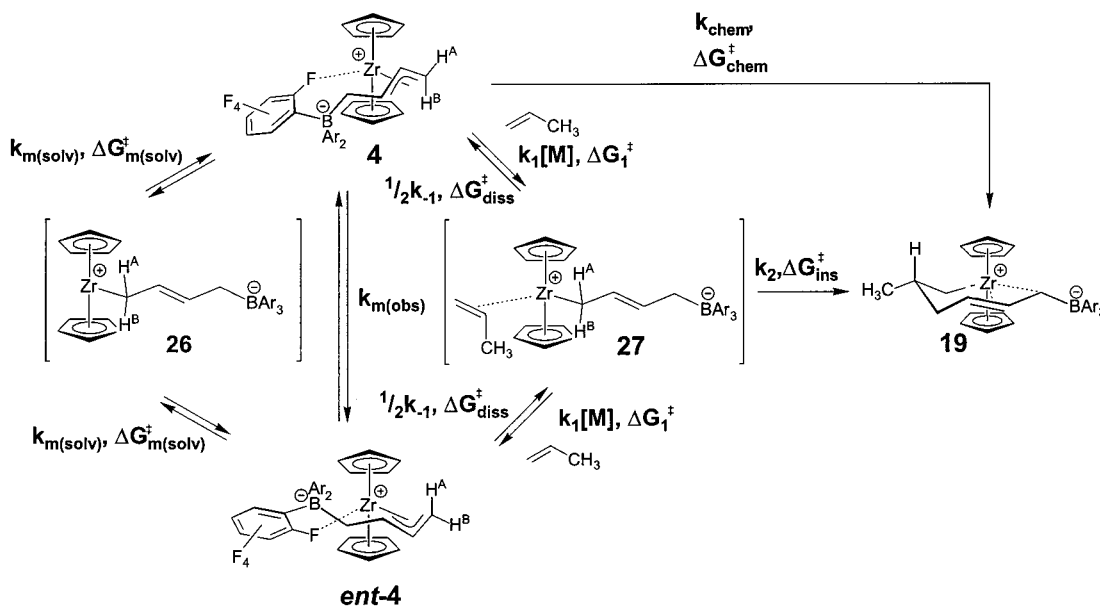


**Table 2. Selected Activation Energy Values Characterizing the Two-Step Alkene Addition/Alkene Insertion Energy Profile in Three Representative Homogeneous Single-Component Betaine Ziegler–Natta Catalyst Systems<sup>a</sup>**

system	$\Delta G_{\text{chem}}^{\ddagger}$	$\Delta G_1^{\ddagger}$	$\Delta\Delta G_2^{\ddagger}$	$k_{-1}/k_2$	$\Delta G_{\text{ins}}^{\ddagger}$
<b>4a<sup>b</sup></b>	18.4(1)	17.1(5)	1.2(5)	8	10.8(9)
	[17.3(1)]	16.5(5)	0.7(5)	3	10.9(9)]
<b>7<sup>c</sup></b>	14.9(1)	13.2(4)	1.7(4)	30	10.6(8)
<b>10<sup>d</sup></b>	19.0(1)	16.5(5)	2.5(5)	80	9.8(9)
	[18.8(1)]	16.4(1)	2.4(1)	80	9.8(5)]

<sup>a</sup> Values given are for reactions with 1-butene [with propene values in brackets]; see Scheme 8 for a definition of the  $k$  and  $\Delta G^{\ddagger}$  values. Gibbs activation energies are given in kilocalories per mole with estimated standard deviations. <sup>b</sup> R = CH<sub>3</sub>, see Scheme 5. <sup>c</sup> See Scheme 2. <sup>d</sup> See Scheme 3.

mol) turned out to be lower than the actual alkene insertion barrier by  $\Delta\Delta G_2^{\ddagger}(253\text{ K}) = 0.7 \pm 0.5$  kcal/mol. Thus, alkene dissociation from the intermediate is favored in this system over alkene insertion by a kinetic ratio of ca. 3:1. Similar values were found for 1-butene or 1-pentene addition/insertion. A very coarse estimate of the actual alkene dissociation barrier (i.e., of the reaction **27a** → **4a**, rate constant  $k_{-1}$ ) was obtained by using the activation energy ( $\Delta G_3^{\ddagger} \approx 7 \pm 0.5$  kcal/mol) of the degenerate rearrangement of the complex  $[(\sigma\text{-allyl})(\pi\text{-allyl})\text{Zr}(\text{CpMe})_2]$ <sup>30</sup> as a model for the  $(\sigma\text{-allyl})$ -to- $(\pi\text{-allyl})$  interconversion<sup>13</sup> during the actual **27a** → **4a** reaction, resulting in  $\Delta G_{\text{diss}}^{\ddagger}(253\text{ K}) \approx 10.2 \pm 0.7$  and  $\Delta G_{\text{ins}}^{\ddagger}(253\text{ K}) \approx 10.9 \pm 0.9$  kcal/mol for propene dissociation over propene insertion at the (MeCp)<sub>2</sub>Zr-derived single-component metallocene betaine Ziegler–Natta catalyst (**4a**). Similar values were obtained for the respective 1-butene- or 1-pentene-derived systems.

Two other representative Ziegler catalyst systems were analogously investigated, namely the dimethylsilylene-bridged ansa-metallocene system **7** (see Scheme 2) and the “constrained geometry” catalyst **10** (see Scheme 3).<sup>29</sup> Both gave qualitatively similar results (see Table 2). The [Cp\*–SiMe<sub>2</sub>–NR]Zr-derived system (**10**) shows an even more pronounced alkene addition/alkene dissociation preequilibrium preceding the actual alkene insertion, with  $k_{\text{diss}}/k_{\text{ins}}$  ratios ranging from ca. 80:1 (propene, 1-butene) to ca. 200:1 (1-hexene). Similar behavior is observed for the [Me<sub>2</sub>Si(C<sub>5</sub>H<sub>4</sub>)<sub>2</sub>]Zr-derived system (**7**). This is by far the most active betaine in this series ( $\Delta G_{\text{chem}}^{\ddagger}(243\text{ K}) = 14.9 \pm 0.1$  kcal/mol for the reaction with 1-butene), but it shows a similar shape of the two-step reaction profile, with the transition state of the first step being energetically located markedly below the actual insertion transition state (e.g.,  $\Delta\Delta G_2^{\ddagger}(243\text{ K}) = 2.1 \pm 0.3$  kcal/mol for 1-pentene insertion). In each case, a coarse estimate of the barriers  $\Delta G_{\text{ins}}^{\ddagger}$  and  $\Delta G_{\text{diss}}^{\ddagger}$  was made. The respective  $(\pi\text{-alkene})\text{Zr}$  complex intermediates lie in wells of similar depths [ $\Delta G_{\text{ins}}^{\ddagger} \approx 10.6 \pm 0.5$ ,  $\Delta G_{\text{diss}}^{\ddagger} \approx 8.9 \pm 0.6$  kcal/mol for **10**,  $9.8 \pm 0.9/7.3 \pm 0.7$  for **7**].

## Conclusions

The addition of the organometallic Lewis acid B(C<sub>6</sub>F<sub>5</sub>)<sub>3</sub> to ( $\eta^4$ -butadiene)group 4 metallocenes and related com-

plexes effectively generates metallocene( $\mu$ -hydrocarbyl)-borate betaines (e.g., **4**) that serve as active homogeneous catalysts for  $\alpha$ -olefin polymerization. In the stable, dormant state, the active metal center in such systems is, in most cases, protected by either an internal ion-pair formation with the –CH<sub>2</sub>–[B] end of the dipole or a weak metal⋯F–C(arene) interaction.<sup>31</sup> In either case, reversible cleavage of this soft metal–ligand coordination combined with a  $\pi$ -allyl ⇌  $\sigma$ -allyl equilibration generates the active species that initiates the catalytic alkene polymerization chain upon contact with a reactive olefin. The system pauses for a short period of time after the very first insertion under specifically chosen conditions, which makes a variety of detailed mechanistic studies at an early stage of the alkene coupling sequence possible, most notable a quantitative evaluation of the alkene addition/insertion energy profile.<sup>32</sup> Further alkene incorporation then leads to an increasing spatial separation of the Cp<sub>2</sub>Zr<sup>+</sup> cation and the –CH<sub>2</sub>B(C<sub>6</sub>F<sub>5</sub>)<sub>3</sub><sup>–</sup> anion end of the dipolar species during the catalyst initiation sequence, until eventually chain transfer takes place, thereby liberating modified hydrocarbyl-tris(pentafluorophenyl)borate anions. The length of their alkyl chains is determined by a variety of specific features of the alkene coupling reaction at the involved active metal catalyst center, which provides the R'–(CHR–CH<sub>2</sub>)<sub>n</sub>–C<sub>4</sub>H<sub>6</sub>–B(C<sub>6</sub>F<sub>5</sub>)<sub>3</sub><sup>–</sup> anions with a specific “memory” of their formation. Among other features, the metallocene betaine Ziegler–Natta catalysts thus obtained are unique in the way that they generate their specifically tailored counteranions during the initiation period. This was demonstrated by a MALDI-TOF-MS study of selected examples.<sup>8</sup>

The metallocene( $\mu$ -butadiene)borate betaines (e.g., **4**) are easily generated, very active homogeneous single-component Ziegler–Natta catalysts, useful for  $\alpha$ -olefin polymerization and copolymerization. They are neutral dipolar systems that are well suited for mechanistic studies, and they bear quite some potential for further catalyst development, including selective involvement of the oligomeric counteranions generated in their initiation phase under the actual catalytic reaction conditions. Several such developments are presently being pursued in our laboratory.<sup>33</sup>

*Most of the studies in our group at Münster were carried out by Bodo Temme, Jörn Karl, and Marc Dahlmann as part of their doctoral work with important contributions by Dr. Roland Fröhlich (X-ray crystal structure analyses), Dr. Klaus Bergander (NMR investigations), and Dr. Heinrich Luftmann (MS studies). It has been a great pleasure for all of us to work together on these projects. Financial support from the Fonds der Chemischen Industrie, the Deutsche Forschungsgemeinschaft, and the NRW Wissenschaftsministerium is gratefully acknowledged.*

## References

- (1) Review: Brintzinger, H.-H.; Fischer, D.; Mülhaupt, R.; Rieger, B.; Waymouth, R. M. Stereospezifische Olefinpolymerisation mit chiralen Metallocenkatalysatoren. *Angew. Chem.* **1995**, *107*, 1255–1283; *Angew. Chem., Int. Ed. Engl.* **1995**, *34*, 1143–1171.
- (2) Jordan, R. F. Chemistry of Cationic Dicyclopentadienyl Group 4 Metal-Alkyl Complexes. *Adv. Organomet. Chem.* **1991**, *32*, 325–387 and references therein.

- (3) Bochmann, M.; Jaggar, A. J.; Nicholls, J. C. Darstellung, Struktur und Olefinpolymerisationsaktivität basenfreier kationischer 14-Elektronen-Alkyltitan- und -zirconiumkomplexe. *Angew. Chem.* **1990**, *102*, 830–832; *Angew. Chem., Int. Ed. Engl.* **1990**, *29*, 780–782.
- (4) Massey, A. G.; Park, A. J. Perfluorophenyl Derivatives of the Elements. I. Tris(pentafluorophenyl)boron. *J. Organomet. Chem.* **1964**, *2*, 245–250.
- (5) Yang, X.; Stern, C. L.; Marks, T. J. Cationic Zirconocene Olefin Polymerization Catalysts Based on the Organo-Lewis Acid Tris(pentafluorophenyl)borane. A Synthetic, Structural, Solution Dynamic, and Polymerization Catalytic Study. *J. Am. Chem. Soc.* **1994**, *116*, 10015–10031.
- (6) Chien, J. C. W.; Tsai, W.-M.; Rausch, M. D. Isospecific Polymerization of Propylene Catalyzed by rac-Ethylenebis(indenyl)methylzirconium "Cation". *J. Am. Chem. Soc.* **1991**, *113*, 8570–8571.
- (7) Review: Sinn, H.; Kaminsky, W. Ziegler–Natta Catalysis. *Adv. Organomet. Chem.* **1980**, *18*, 99–149.
- (8) Temme, B.; Erker, G.; Karl, J.; Luftmann, H.; Fröhlich, R.; Kotila, S. Reaktion von (Butadien)zirconocen mit Tris(pentafluorophenyl)boran—ein neuer Weg zur Herstellung Alumoxan-freier Metallocen-Ziegler-Katalysatoren. *Angew. Chem.* **1995**, *107*, 1867–1869; *Angew. Chem., Int. Ed. Engl.* **1995**, *34*, 1755–1757.
- (9) Reviews: Yasuda, H.; Tatsumi, K.; Nakamura, A. Unique Chemical Behavior and Bonding of Early-Transition-Metal-Diene Complexes. *Acc. Chem. Res.* **1985**, *18*, 120–126. Erker, G.; Krüger, C.; Müller, G. The Remarkable Features of ( $\eta^4$ -Conjugated Diene)-zirconocene and -hafnocene Complexes. *Adv. Organomet. Chem.* **1985**, *24*, 1–39.
- (10) For recent examples of related organometallic betaine systems, see, e.g.: Hlatky, G. G.; Turner, H.; Eckmann, R. R. Ionic, Base-Free Zirconocene Catalysts for Ethylene Polymerization. *J. Am. Chem. Soc.* **1989**, *111*, 2728–2729. Pindado, G. J.; Thornton-Pett, M.; Bochmann, M. Zirconium and hafnium diene and dienyl half-sandwich complexes: synthesis, polymerization catalysis and deactivation pathways. *J. Chem. Soc., Dalton Trans.* **1997**, 3115–3127. Sun, Y.; Piers, W. E.; Rettig, S. J. Zwitterionic alkene polymerization catalyst derived from  $\text{Cp}_2\text{Zr}(\eta^2\text{-C}_2\text{H}_4)\text{PPh}_2\text{Me}$  and  $\text{B}(\text{C}_6\text{F}_5)_3$ . *J. Chem. Soc., Chem. Commun.* **1998**, 127–128. Cowley, A. H.; Hair, G. S.; McBurnett, B. G.; Jones, R. A. Novel Zwitterionic complexes of Ti(IV) via reaction of Lewis acids  $\text{M}(\text{C}_6\text{F}_5)_3$  (M = B, Al) with a titanium diene complex ( $\eta^5\text{-C}_5\text{Me}_4\text{SiMe}_2\text{N}^i\text{Bu}$ )Ti(1,3-pentadiene). *J. Chem. Soc., Chem. Commun.* **1999**, 437–438. Reviews: Piers, W. E.; Chivers, T. Pentafluorophenylboranes: from obscurity to applications. *Chem. Soc. Rev.* **1997**, 345–354. Piers, W. E. Zwitterionic Metallocenes. *Chem. Eur. J.* **1998**, 13–18.
- (11) Erker, G.; Wicher, J.; Engel, K.; Krüger, C. (s-trans- $\eta^4$ -Dien)-zirconocen-Komplexe. *Chem. Ber.* **1982**, *115*, 3300–3309. Erker, G.; Engel, K.; Krüger, C.; Chiang, A.-P. Reaktionsverhalten und Struktur von (s-cis-1,3-Dien)zirconocen-Komplexen. *Chem. Ber.* **1982**, *115*, 3311–3323. Yasuda, H.; Kajihara, Y.; Mashima, K.; Nagasuna, K.; Lee, K.; Nakamura, A. 1,3-Diene Complexes of Zirconium and Hafnium Prepared by the Reaction of Etylilmagnesium with  $\text{MCl}_2\text{Cp}_2$ . A Remarkable Difference between the Zirconium and Hafnium Analogues as Revealed by  $^1\text{H}$  NMR and Electronic Spectra. *Organometallics* **1982**, *1*, 388–396.
- (12) Brintzinger, H. H.; Bartell, L. S. Extended Hückel Calculations Related to the Chemistry of Titanocene. *J. Am. Chem. Soc.* **1970**, *92*, 1105–1107. Lauher, W.; Hoffmann, R. Structure and Chemistry of Bis(cyclopentadienyl)- $\text{ML}_n$  Complexes. *J. Am. Chem. Soc.* **1976**, *98*, 1729–1742.
- (13) Hoffmann, E. G.; Kallweit, R.; Schroth, G.; Seevogel, K.; Stempfle, W.; Wilke, G. IR- und  $^1\text{H}$ -NMR-spektroskopische Untersuchungen an Zirkon- und Hafniumallylen. *J. Organomet. Chem.* **1975**, *97*, 183–202.
- (14) Karl, J.; Erker, G.; Fröhlich, R. Internal Fluorocarbon Coordination as a Tool für the Protection of Active Catalytic Sites: Experimental Characterization of the Zr–F–C Interaction in the Group 4 Metallocene(butadiene)/ $\text{B}(\text{C}_6\text{F}_5)_3$  Betaine Ziegler Catalyst Systems. *J. Am. Chem. Soc.* **1997**, *119*, 11165–11173.
- (15) Dahlmann, M.; Erker, G.; Fröhlich, R.; Meyer, O. Structural Dichotomy in Single-Component Ziegler Catalyst Systems: Characterization of Zr–F and Zr–C Bonded Structural Types of Group 4 Metallocene  $[\text{C}_4\text{H}_6\text{-B}(\text{C}_6\text{F}_5)_3]\text{Betaines}$ . *Organometallics* **2000**, *19*, 2956–2967.
- (16) Shapiro, P. J.; Bunel, E. E.; Schaefer, W. P.; Bercaw, J. E.  $\{[(\eta^5\text{-C}_5\text{Me}_4)\text{Me}_2\text{Si}(\eta^1\text{-NCMe}_3)](\text{PMe}_2)\text{Sch}\}_2$ : A Unique Example of a Single-Component  $\alpha$ -Olefin Polymerization Catalyst. *Organometallics* **1990**, *9*, 867–869. Review: McKnight, A. L.; Waymouth, R. M. Group 4 ansa-Cyclopentadienyl-Amido Catalysts for Olefin Polymerization. *Chem. Rev.* **1998**, *98*, 2587–2598.
- (17) Dahlmann, M.; Schottek, J.; Fröhlich, R.; Kunz, D.; Nissinen, M.; Erker, G.; Fink, G.; Kleinschmidt, R. Structural characterization of  $\text{M}(\text{s-cis-}\eta^4\text{-C}_4\text{H}_6)(\text{Me}_4\text{C}_5\text{SiMe}_2\text{NR})$  (M = Ti or Zr, R =  $\text{CMe}_3$  or  $\text{CHCMe}(\text{1-C}_{10}\text{H}_7)$ ). *J. Chem. Soc., Dalton Trans.* **2000**, 1881–1886. Devore, D. D.; Timmers, F. J.; Hasha, D. L.; Rosen, R. K.; Marks, T. J.; Deck, P. A.; Stern, C. L. Constrained-Geometry Titanium(II) Diene Complexes. Structural Diversity and Olefin Polymerization Activity. *Organometallics* **1995**, *14*, 3132–3134.
- (18) Yasuda, H.; Tatsumi, K.; Okamoto, T.; Mashima, K.; Lee, K.; Nakamura, A.; Kai, Y.; Kanehisa, N.; Kasai, N. Unique Bonding and Geometry in  $\eta$ -Cyclopentadienyltantalum-Diene Complexes. Preparation, X-ray Structural Analyses, and EHMO Calculations. *J. Am. Chem. Soc.* **1985**, *107*, 2410–2422.
- (19) Karl, J.; Erker, G.; Fröhlich, R.  $\text{Cp}_2^*\text{Zr}(\mu\text{-C}_4\text{H}_6)\text{B}(\text{C}_6\text{F}_5)_3$ , a first example of a stable unbridged homogeneous metallocene-betaine Ziegler catalyst system. *J. Organomet. Chem.* **1997**, *535*, 59–62.
- (20) Dahlmann, M.; Fröhlich, R.; Erker, G. Reaction of a Zirconocene-(butadiene)borate-Betaine Single-Component Ziegler Catalyst with Trimethylphosphane. *Eur. J. Inorg. Chem.* **2000**, 1789–1793. Green, J. C.; Green, M. L. H.; Taylor, G. C.; Saunders, J. Studies on ansa-zirconocene-butadiene derivatives. *J. Chem. Soc., Dalton Trans.* **2000**, 317–327.
- (21) Temme, B.; Karl, J.; Erker, G. Observing a Homogeneous Ziegler Catalyst Precursor at Work: Insertion Reactions into the Zirconium–Carbon Bond of the (Butadiene)ZrCp<sub>2</sub>B(C<sub>6</sub>F<sub>5</sub>)<sub>3</sub> Addition Product. *Chem. Eur. J.* **1996**, *2*, 919–924. Karl, J.; Erker, G. Evidence for Internal Ion Pair Formation upon Insertion of Reactive Alkenes in the Zirconium–Carbon Bond of the  $\text{Cp}_2\text{Zr}(\mu\text{-C}_4\text{H}_6)\text{B}(\text{C}_6\text{F}_5)_3$  Metallocene-Boron-Betaine Ziegler Catalyst System. *Chem. Ber./Recl.* **1997**, *130*, 1261–1267. Karl, J.; Erker, G. Observation of the primary Zr–C insertion products in the reaction of the (butadiene)zirconocene/ $\text{B}(\text{C}_6\text{F}_5)_3$ -betaine Ziegler catalyst system with reactive alkynes. *J. Mol. Catal. A* **1998**, *128*, 85–102.
- (22) For functionally related model systems see, e.g.: Pellecchia, C.; Grassi, A.; Zambelli, A. Single Insertion of  $\alpha$ -Olefins into the Cationic Complex  $[\text{Zr}(\text{CH}_2\text{Ph})_3]^+$  Affording Isolable  $[\text{Zr}(\text{CH}_2\text{Ph})_2(\text{CH}_2\text{CHRCH}_2\text{Ph})]^+$  Adducts: A Model for the Insertion Mechanism in Ziegler–Natta Polymerization. *Organometallics* **1994**, *13*, 298–302. Dagorne, S.; Rodewald, S.; Jordan, R. F. Stereoselective Propene Insertion Reactions of rac-(EB)Zr( $\eta^2$ -pyridyl)<sup>+</sup> Complexes. *Organometallics* **1997**, *16*, 5541–5555.
- (23) Wu, Z.; Jordan, R. F. Models for the Elusive  $\text{Cp}_2\text{Zr}(\text{R})(\text{olefin})^+$  Characterization of the d<sup>0</sup>-Metal Olefin Complex  $\text{Cp}_2\text{Zr}(\text{OCMe}_2\text{-CH}_2\text{CH}_2\text{CH}=\text{CH}_2)^+$ . *J. Am. Chem. Soc.* **1995**, *117*, 5867–5868. Casey, C. P.; Hallenbeck, S. L.; Pollock, D. W.; Landis, C. R. Synthesis and Spectroscopic Characterization of the d<sup>0</sup> Transition Metal-Alkyl-Alkene Complex  $\text{Cp}_2^*\text{YCH}_2\text{CH}_2\text{C}(\text{CH}_3)_2\text{CH}=\text{CH}_2$ . *J. Am. Chem. Soc.* **1995**, *117*, 9770–9771. Galakhov, M. V.; Heinz, G.; Royo, P. Intramolecular coordination of an alkene to a mixed dicyclopentadienyl benzyl zirconium cation studied by NMR spectroscopy. *J. Chem. Soc., Chem. Commun.* **1998**, 17–18.
- (24) Dahlmann, M.; Erker, G.; Nissinen, M.; Fröhlich, R. Direct Experimental Observation of the Stereochemistry of the First Propene Insertion Step at an Active Homogeneous Single Component Metallocene Ziegler Catalyst. *J. Am. Chem. Soc.* **1999**, *121*, 2820–2828.
- (25) Corradini, P.; Barone, V.; Fusco, R.; Guerra, G. Steric Control in Ziegler–Natta Catalysts: An Analysis of Nonbonded Interactions at Model Catalytic Sites. *J. Catal.* **1982**, *77*, 32–42. Corradini, P.; Barone, V.; Guerra, G. Steric Control in the First Step of the Isospecific Ziegler–Natta Polymerization of Propene. *Macromolecules* **1982**, *15*, 1242–1245. Sacchi, M. C.; Locatelli, P.; Tritto, I.  $^{13}\text{C}$  NMR analysis of ethyl chain-end groups: A method for active site investigation in Ziegler–Natta Catalysis. *Makromol. Chem.* **1989**, *190*, 139–143.
- (26) Longo, P.; Grassi, A.; Pellecchia, C.; Zambelli, A.  $^{13}\text{C}$ -Enriched End Groups of Isotactic Polypropylene and Poly(1-butene) Prepared in the Presence of Ethylenediindenyl dimethyltitanium and Methylalumoxane. *Macromolecules* **1987**, *20*, 1015–1018. Gilchrist, J. H.; Bercaw, J. E. New NMR Spectroscopic Probe of the Absolute Stereoselectivity for Metal-Hydride and Metal-Alkyl Additions to the Carbon–Carbon Double Bond. Demonstration with a Single-Component, Isospecific Ziegler–Natta  $\alpha$ -Olefin Polymerization Catalyst. *J. Am. Chem. Soc.* **1996**, *118*, 12021–12028. Sacchi, M. C.; Barsties, E.; Tritto, I.; Locatelli, P.; Brintzinger, H.-H.; Stehling, U. Stereochemistry of First Monomer Insertion into Metal-Methyl Bond: A Tool for Evaluating Ligand-Monomer Interactions in Propene Polymerization with Metallocene Catalysts. *Macromolecules* **1997**, *30*, 3955–3957.
- (27) For theoretical studies concerning the energy profile of homogeneous Ziegler systems, see, e.g.: Margl, P.; Deng, L.; Ziegler, T. A Unified View of Ethylene Polymerization by d<sup>0</sup> and d<sup>0m</sup> Transition Metals. 1. Precursor Compounds and Olefin Uptake



- Energetics. *Organometallics* **1998**, *17*, 933–946. Froese, R. D. J.; Musaev, D. G.; Morokuma, K. Theoretical studies of the Cp<sub>2</sub>ZrR<sup>+</sup>-catalyzed propylene polymerization reactions and a comparison with ethylene polymerization. *J. Mol. Struct. (THEOCHEM)* **1999**, *461–462*, 121–135 and references therein.
- (28) Karl, J.; Dahlmann, M.; Erker, G.; Bergander, K. Arriving at an Experimental Estimate of the Intrinsic Activation Barrier of Olefin Insertion into the Zr–C Bond of an Active Metallocene Ziegler Catalyst. *J. Am. Chem. Soc.* **1998**, *120*, 5643–5652.
- (29) Dahlmann, M.; Erker, G.; Bergander, K. Experimental Characterization of the Alkene-Addition/Insertion Energy Profile at Homogeneous Group 4 Metal Ziegler-Type Catalysts. *J. Am. Chem. Soc.* **2000**, *122*, 7986–7998.
- (30) Erker, G.; Berg, K.; Angermund, K.; Krüger, C. CpZr(allyl)<sub>3</sub>: The Molecular Structure of a  $\pi$ - and  $\sigma$ -Dynamic Allyl Transition Metal Complex. *Organometallics* **1987**, *6*, 2620–2621.
- (31) Plenio, H. The Coordination Chemistry of the CF Units in Fluorocarbons. *Chem. Rev.* **1997**, *97*, 3363–3384.
- (32) Casey, C. P.; Carpenetti, D. W., II; Sakurai, H. Observation of Zwitterionic d<sup>0</sup> Zirconium-Alkyl-Alkene Chelates: Models for Intermediates in Metallocene-Catalyzed Alkene Polymerizations. *J. Am. Chem. Soc.* **1999**, *121*, 9483–9484.
- (33) Kehr, G.; Fröhlich, R.; Wibbeling, B.; Erker, G. (N-Pyrrolyl)B(C<sub>6</sub>F<sub>5</sub>)<sub>2</sub>—A New Organometallic Lewis Acid for the Generation of Group 4 Metallocene Cation Complexes. *Chem. Eur. J.* **2000**, *6*, 258–266.

AR9800183